EVALUATION METHOD OF THE COUPLING FACTORS BETWEEN CAVITIES IN THE ARES CAVITY SYSTEM

Takaaki Yamaguchi*, Tetsuya Kobayashi, Tetsuo Abe
High Energy Accelerator Research Organization, Tsukuba, Japan

Abstract

The ARES cavity has been used in SuperKEKB accelerator for suppressing coupled-bunch instabilities caused by the accelerating mode. The important parameters characterizing the ARES cavity system are the coupling factors between cavities. However, it is not straightforward to evaluate the coupling factors in the case of the ARES cavity. This is because the cavities of which the ARES cavity system consists have different cavity geometries. Then, we developed a method of evaluating the inter-cavity couplings using eigenmode simulations and an equivalent circuit model. In this paper, we discuss this method and evaluate the inter-cavity coupling factors for the ARES cavity.

INTRODUCTION

In extremely high-intensity storage rings such as SuperKEKB accelerator, an electron-positron collider, the accelerating mode causes coupled-bunch instabilities. In order to suppress them in SuperKEKB, the normal-conducting ARES (Accelerator Resonantly-coupled with Energy Storage) cavities [1–4] have been used in addition to the superconducting cavities. The ARES cavity consists of an accelerating cavity (A-cavity), a coupling cavity (C-cavity), and an energy storage cavity (S-cavity). The A-cavity is resonantly coupled with the S-cavity via the C-cavity that is located between the A- and S-cavity. Because of large stored energy in the S-cavity, the optimum detuning frequency can be decreased, which prevents the resonant frequency of the accelerating mode from crossing the resonances of coupled-bunch modes. While the $\pi/2$ mode is used for beam acceleration, the parasitic 0 and π modes are heavily damped by the coupling cavity damper (C-damper). The C-damper is a coaxial antenna-type damper installed in the C-cavity.

The ARES cavity was developed in 1990's [1–4] for the KEKB, the predecessor of SuperKEKB. Around that time, it was the dawn of three-dimensional electromagnetic simulations [5]. Recently, we started simulation study on the ARES cavity, again. The aim of this study is to reconsider the tolerance of the ARES cavity to twice as high beam current in SuperKEKB as that in KEKB. In addition, the modern simulation software and computers enable us to simulate electromagnetic field much more precisely than they could in 1990's. Then, it is meaningful to recalculate some important properties of the ARES cavity. We have conducted the simulation study on the ARES cavity using CST Studio Suite [6], and recently reported a part of the results in IPAC 2025 [7] that is on the C-damper power leakage of the accelerating $\pi/2$ mode. This paper is a series of the study in [7], and here we focus on the inter-cavity coupling factors.

To characterize the ARES cavity system, the coupling factors between cavities (inter-cavity coupling factors) are important. The cavity response function of the ARES cavity depends on these factors. Thus, the inter-cavity coupling factors affect the transient beam loading effect caused by un-uniform filling patterns [8] and the C-damper power leak of the $\pi/2$ mode [7]. For these purposes, evaluation of the accurate coupling factors are indispensable for predicting these phenomena.

In typical multi-cell cavities where all the cells have the same geometry, the inter-cavity coupling factor can be derived from the frequency difference of the mode frequencies [9]. However, in the case of the ARES cavity, the A-, C-, and S-cavities have largely different geometries and cavity parameters. This makes it difficult to evaluate the inter-cavity coupling factors.

Then, we newly developed a method to evaluate the inter-cavity coupling factors using electromagnetic eigenmode simulation and an equivalent circuit model of a three-coupled-cavity system. In this paper, we first analyse the equivalent circuit model of the ARES cavity and consider the method of determining the inter-cavity coupling factors. Second, we conduct electromagnetic simulations of the ARES cavity and evaluate the coupling factors.

EVALUATION METHOD OF INTER-CAVITY COUPLING FACTORS

Equivalent circuit model of the ARES cavity system

According to the equivalent circuit model of the ARES cavity system, the RF voltages $(x_\mathrm{a}, x_\mathrm{c}, x_\mathrm{s})$ generated in the A-, C-, and S-cavities are described by the following simultaneous differential equations [1, 2][1]:

$$\begin{aligned}
&\ddot{x}_\mathrm{a} + 2\alpha_\mathrm{a}\dot{x}_\mathrm{a} + \omega_\mathrm{a}^2 x_\mathrm{a} = -k_\mathrm{a}\ddot{x}_\mathrm{c} - 2k_{\mathrm{L,a}}\frac{\mathrm{d}i_\mathrm{b}}{\mathrm{d}t}\,,\\
&\ddot{x}_\mathrm{c} + 2\alpha_\mathrm{c}\dot{x}_\mathrm{c} + \omega_\mathrm{c}^2 x_\mathrm{c} = -k_\mathrm{a}\ddot{x}_\mathrm{a} - k_\mathrm{s}\ddot{x}_\mathrm{s}\,,\\
&\ddot{x}_\mathrm{s} + 2\alpha_\mathrm{s}\dot{x}_\mathrm{s} + \omega_\mathrm{s}^2 x_\mathrm{s} = -k_\mathrm{s}\ddot{x}_\mathrm{c} + 2k_{\mathrm{L,a}}\frac{\mathrm{d}i_\mathrm{g}}{\mathrm{d}t}\,.
\end{aligned} \tag{1}$$

where ω_a, ω_c, and ω_s are the resonant frequencies, α_a, α_c, and α_s are the damping rates of the isolated A-, C-, and S-cavities, respectively, i_b is the frequency component around the RF frequency of the beam current, i_g is the generator

* yamaguc@post.kek.jp

[1] In [1] and [2], the definitions of k_s and k_a differ by a factor 2. We use the same definition with that in [2].

current, k_a is the coupling factor between the A- and C-cavity, k_s is that between the S- and C-cavity, and $k_{L,a}$ is the loss factor of the isolated A-cavity. Denoting the unloaded Q's of the isolated A-, C-, and S-cavities as Q_a, Q_c, and Q_s, respectively, the damping rates are given by

$$\alpha_a = \frac{\omega_a}{2Q_a}, \tag{2}$$

$$\alpha_c = \frac{\omega_c(1+\beta_c)}{2Q_c} = \frac{\omega_c}{2Q_{L,c}}, \tag{3}$$

$$\alpha_s = \frac{\omega_s(1+\beta_s)}{2Q_s} = \frac{\omega_s}{2Q_{L,s}}, \tag{4}$$

where β_c and β_s are the external coupling factors, and $Q_{L,c}$ and $Q_{L,s}$ are the loaded Q's of the isolated C- and S-cavities, respectively. Here, β_c is the coupling factor to the C-damper and β_s is that to an input coupler. It should be noted that the parameters ω_i, α_i, Q_i (for $i = a, c, s$), β_i, $Q_{L,i}$ (for $i = c, s$), and $k_{L,a}$ are those in the case there are no couplings between cavities. The C-cavity is heavily-damped, and then $\alpha_c \gg \alpha_a, \alpha_s$.

Eigenmodes

Laplace-transforming Eq. (1), we have

$$A(s)\mathbf{X}(s) = 2k_{L,a}s\mathbf{E}(s) \tag{5}$$

where

$$\mathbf{X}(s) = (X_a(s), X_c(s), X_s(s))^T, \tag{6}$$

$$\mathbf{E}(s) = \left(-I_b(s),\ 0,\ I_g(s)\right)^T, \tag{7}$$

$$A(s) = \begin{pmatrix} d_a(s) & k_a s^2 & 0 \\ k_a s^2 & d_c(s) & k_s s^2 \\ 0 & k_s s^2 & d_s(s) \end{pmatrix}, \tag{8}$$

$$d_i(s) = s^2 + 2\alpha_i s + \omega_i^2, \tag{9}$$

$X_i(s)$ $(i = a, c, s)$, $I_b(s)$, and $I_g(s)$ are the Laplace transforms of $x_i(t)$ $(i = a, c, s)$, $i_b(t)$, and $i_g(t)$, respectively. Let us consider the case where the excitation term is zero, namely $\mathbf{E}(s) = \mathbf{0}$. In this case, to obtain non-trivial solution $\mathbf{X} \neq \mathbf{0}$, we need

$$D(s) \equiv \det A(s) = 0. \tag{10}$$

The determinant $D(s)$ is a sixth-degree polynomial of s:

$$\begin{aligned} D(s) &= d_a(s)d_c(s)d_s(s) - s^4\left[k_s^2 d_a(s) + k_a^2 d_s(s)\right] \\ &= a_6 s^6 + a_5 s^5 + a_4 s^4 + a_3 s^3 + a_2 s^2 + a_1 s + a_0 \end{aligned} \tag{11}$$

with

$$\begin{aligned} a_6 &= 1 - k_s^2 - k_a^2, \\ a_5 &= 2(1-k_a^2)\alpha_s + 2\alpha_c + 2(1-k_s^2)\alpha_a, \\ a_4 &= 4\alpha_s\alpha_c + 4\alpha_c\alpha_a + 4\alpha_a\alpha_s \\ &\quad + (1-k_a^2)\omega_s^2 + \omega_c^2 + (1-k_s^2)\omega_a^2, \\ a_3 &= 2(\alpha_c+\alpha_a)\omega_s^2 + 2(\alpha_a+\alpha_s)\omega_c^2 + 2(\alpha_s+\alpha_c)\omega_a^2 \\ &\quad + 8\alpha_a\alpha_c\alpha_s, \\ a_2 &= 4\alpha_c\alpha_a\omega_s^2 + 4\alpha_a\alpha_s\omega_c^2 + 4\alpha_s\alpha_c\omega_a^2 \\ &\quad + \omega_s^2\omega_c^2 + \omega_c^2\omega_a^2 + \omega_a^2\omega_s^2, \\ a_1 &= 2\alpha_a\omega_s^2\omega_c^2 + 2\alpha_s\omega_c^2\omega_a^2 + 2\alpha_c\omega_a^2\omega_s^2, \\ a_0 &= \omega_s^2\omega_c^2\omega_a^2. \end{aligned}$$

The solutions of the characteristic equation (10) correspond to the complex eigenvalues of 0, $\pi/2$, and π modes:

$$s_\mu = -\alpha_\mu + j\overline{\omega}_\mu, \qquad \mu = 0,\ \pi/2,\ \pi \tag{12}$$

where α_μ and $\overline{\omega}_\mu (> 0)$ are the damping rate and eigenfrequency of mode μ, respectively. Note that their complex conjugates s_μ^* are also the solutions of Eq. (10).

First, in the simplest case of $\alpha_a = \alpha_c = \alpha_s = 0$ and $\omega_a = \omega_c = \omega_s = \omega$, the eigenvalue s_μ and eigenvector $\mathbf{X}_\mu$ are analytically calculated as [1]

$$s_0 = \frac{j\omega}{\sqrt{1+\sqrt{k_s^2+k_a^2}}}, \quad \mathbf{X}_0 = A\begin{pmatrix} k_a \\ \sqrt{k_a^2+k_s^2} \\ k_s \end{pmatrix}, \tag{13}$$

$$s_{\frac{\pi}{2}} = j\omega, \qquad \mathbf{X}_{\frac{\pi}{2}} = A\begin{pmatrix} k_s \\ 0 \\ -k_a \end{pmatrix}, \tag{14}$$

$$s_\pi = \frac{j\omega}{\sqrt{1-\sqrt{k_s^2+k_a^2}}}, \quad \mathbf{X}_\pi = A\begin{pmatrix} -k_a \\ \sqrt{k_a^2+k_s^2} \\ -k_s \end{pmatrix}, \tag{15}$$

where A is an arbitrary complex value. For the ARES cavity, $k_a, k_s > 0$ and $k_a, k_s \ll 1$.

Next, we consider the $\pi/2$ mode with more general case where each cavity has a non-zero damping rate $(\alpha_a, \alpha_c, \alpha_s)$ and a different resonant frequency as

$$\omega_i = \omega + \Delta\omega_i, \quad i = a,\ c,\ s \tag{16}$$

where $\Delta\omega_i$ is a small frequency offset $(\Delta\omega_i/\omega \ll 1)$. We assume the eigenvalue of the $\pi/2$ mode as

$$s_{\frac{\pi}{2}} = j\omega + \sigma_{\frac{\pi}{2}}, \qquad |\sigma_{\frac{\pi}{2}}| \ll \omega \tag{17}$$

where $\sigma_{\frac{\pi}{2}}$ is a small perturbation of the eigenvalue. From $D(j\omega + \sigma_{\frac{\pi}{2}}) = 0$, we have [1]

$$\sigma_{\frac{\pi}{2}} \approx -\frac{k_s^2\alpha_a + k_a^2\alpha_s}{k_s^2+k_a^2} + j\frac{k_s^2\Delta\omega_a + k_a^2\Delta\omega_s}{k_s^2+k_a^2}. \tag{18}$$

From Eq. (18), the frequency offset of the $\pi/2$ mode is linearly dependent on the frequency offsets of the A- and S-cavity as

$$\Delta\omega_{\frac{\pi}{2}} = \overline{\omega}_{\frac{\pi}{2}} - \omega = \frac{k_s^2\Delta\omega_a + k_a^2\Delta\omega_s}{k_s^2+k_a^2}. \tag{19}$$

Then, we can obtain the ratio k_a^2/k_s^2 by investigating the dependence of $\Delta\omega_{\frac{\pi}{2}}$ on $\Delta\omega_a$ and $\Delta\omega_s$ in eigenmode simulations. However, to determine k_s and k_a, we must calculate 0 and π modes too.

In a similar way to Eq. (17), we write the eigenvalues of 0 and π modes as

$$s_\mu = j\omega + \sigma_\mu, \quad \mu = 0, \pi. \tag{20}$$

Assuming that $\sqrt{k_s^2 + k_a^2}\omega \gg |\Delta\omega_a|, |\Delta\omega_s|, \alpha_a, \alpha_s$, the characteristic equations $D(j\omega + \sigma_\mu) = 0$ for $\mu = 0, \pi$ give

$$\sigma_\mu \approx \frac{1}{2}\left[-\alpha_c\left(1 \pm \frac{\Delta\omega_c}{\sqrt{(k_s^2 + k_a^2)\omega^2 - \alpha_c^2}}\right) + j\left(\Delta\omega_c \pm \sqrt{(k_s^2 + k_a^2)\omega^2 - \alpha_c^2}\right)\right] \text{ for } \begin{cases}\pi \text{ mode} \\ 0 \text{ mode}\end{cases} \tag{21}$$

The damping rates α_μ and the resonant frequencies $\overline{\omega}_\mu$ are

$$\alpha_\mu \approx \frac{1}{2}\alpha_c\left(1 \pm \frac{\Delta\omega_c}{\sqrt{(k_s^2 + k_a^2)\omega^2 - \alpha_c^2}}\right) \text{ for } \begin{cases}\pi \text{ mode}, \\ 0 \text{ mode}, \end{cases} \tag{22}$$

$$\overline{\omega}_\mu \approx \omega + \frac{\Delta\omega_c \pm \sqrt{(k_s^2 + k_a^2)\omega^2 - \alpha_c^2}}{2} \text{ for } \begin{cases}\pi \text{ mode}, \\ 0 \text{ mode}. \end{cases} \tag{23}$$

From this result, we can derive the value $k_s^2 + k_a^2$ from the frequencies and damping rates of the 0 and π modes as

$$k_s^2 + k_a^2 = \frac{(\overline{\omega}_\pi - \overline{\omega}_0)^2 + (\alpha_\pi + \alpha_0)^2}{\omega^2}. \tag{24}$$

Hence, we can derive the values of k_s and k_a from the complex mode frequencies of 0, $\pi/2$, and π modes.

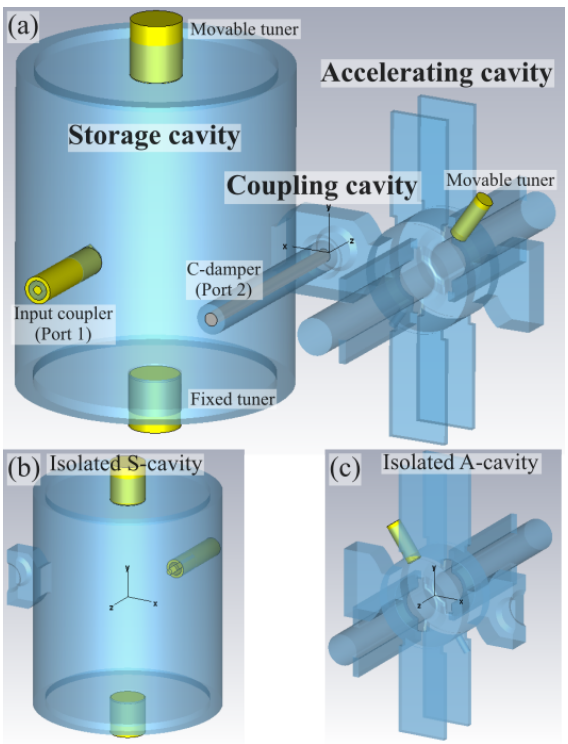

Figure 1: Three-dimensional models for the ARES cavity.

EIGENMODE SIMULATION

We applied the method discussed in the previous section to derive the inter-cavity coupling factors of the ARES cavity. Figure 1 shows the three-dimensional models of the ARES cavity for CST Studio Suite. Figure 1(a) is the full model of the ARES cavity, and Figs. 1(b) and (c) are the isolated models of the S- and A-cavities, respectively. The ARES cavity has totally two movable frequency tuners in the A- and S-cavity each, which are controlled by auto-tuner controllers. We set the terminations of the input coupler in the S-cavity and the C-damper in the C-cavity as Waveguide Ports. In this setting, the terminations are ideally matched-terminated.

Isolated A- and S-cavities [7]

First, we calculated the resonant frequencies of the A- and S-cavities as the functions of tuner positions using CST MW Studio, Eigenmode Solver. This simulation is needed to convert the positions (d_a and d_s) of the movable tuners in the A- and S-cavity to the frequencies ω_a and ω_s. In this simulation, we used the isolated cavity models in Figs. 1(b) and (c). In those models, the ARES cavity was separated into two volumes at the centre of the C-cavity, and the C-damper was omitted. The boundary plane of the isolated cavities is electrically-shorted.

The calculated resonant frequency changes Δf_i ($i = a, s$) are shown in Fig. 2 as the functions of the tuner position d_i. The tops of the tuners are flush with cavity surface at $d_i = 0$. The frequency changes are defined as $\Delta f_i = f_i - f$ where $f_i = \omega_i/(2\pi)$ is the resonant frequency calculated by the Eigenmode solver and $f = \omega/(2\pi) = 508.877$ MHz (RF frequency in SuperKEKB). The circles show the simulated results and the dashed line shows the quadratic fit.

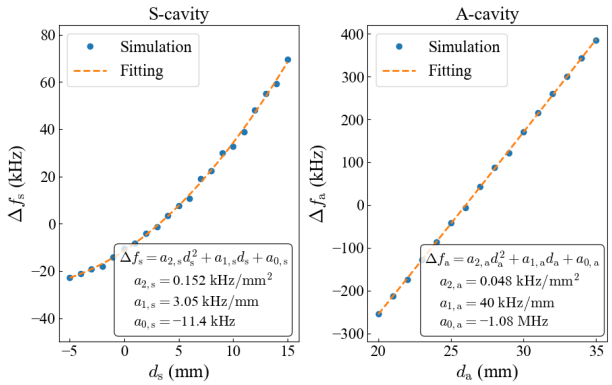

Figure 2: Frequency changes of S- and A-cavities as the functions of tuner positions.

$\pi/2$ mode [7]

Next, using the full model of the ARES cavity in Fig. 1(a), we simulated the frequency $\overline{f}_{\frac{\pi}{2}} = \overline{\omega}_{\frac{\pi}{2}}/(2\pi)$ of the $\pi/2$ mode with moving two tuners independently. Moving the tuners is equivalent to changing the frequencies of ω_a and ω_s.

The simulated $\pi/2$-mode frequency change $\Delta f_{\frac{\pi}{2}} = \overline{f}_{\frac{\pi}{2}} - f$ at fixed Δf_s is shown in Fig. 3 with circles and triangles as

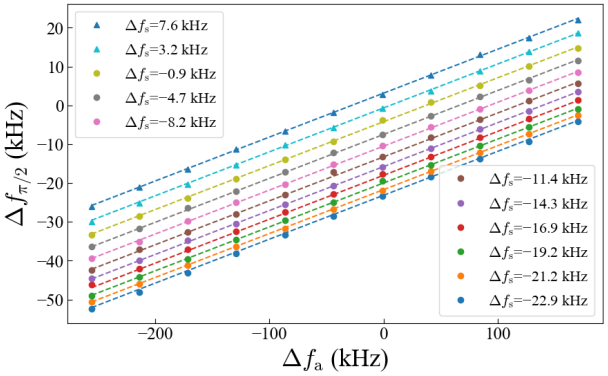

Figure 3: Frequency change of the $\pi/2$ mode at fixed Δf_s as the function of Δf_a.

the function of Δf_a. The positions of the movable tuners in S- and A-cavity were changed as $d_s = -5, -4, \cdots, 4, 5$ mm and $d_a = 20, 21, \cdots, 29, 30$ mm, respectively. Taking into account Eq. (19), we fitted the simulated results to the following function

$$\Delta f_{\frac{\pi}{2}} = c_a \Delta f_a + c_s \Delta f_s + c_0 \,. \tag{25}$$

The fitted result is shown with dashed lines in Fig. 3 and the optimum coefficients are

$$c_a = 0.113, \quad c_s = 0.862, \quad c_0 = -3.43\,\text{kHz}\,. \tag{26}$$

From Eq. (19), the ratio k_a^2/k_s^2 is calculated as

$$\frac{k_a^2}{k_s^2} = \frac{c_s}{c_a} = 7.619\,. \tag{27}$$

0 *and* π *modes*

Finally, we simulated the 0 and π modes. The positions of the movable tuners were set to satisfy $\Delta f_a = \Delta f_s = 0$. The simulated resonant frequencies and loaded Q's of 0, $\pi/2$, and π modes are shown in Table 1.

Here, we find that there are approximately 10% differences between $|\overline{\omega}_0 - \omega|$ and $|\overline{\omega}_\pi - \omega|$ and between $Q_{L,0}$ and $Q_{L,\pi}$. From Eqs. (22) and (23), it indicates that the C-cavity has a non-zero frequency offset $\Delta\omega_c = 2\pi\Delta f_c$. It is difficult to exactly simulate the frequency ω_c of the C-cavity by the same way with the S- and A-cavities using isolated cavity models. This is because the C-cavity has relatively large openings compared with its volume for coupling with S- and A-cavities, and then the resonant frequency should be non-negligibly changed when the openings are electrically-shorted. From Eqs. (22) and (23), we can estimate the frequency and damping rate of the C-cavity as

$$\alpha_c = \alpha_\pi + \alpha_0, \tag{28}$$

$$\Delta\omega_c = \overline{\omega}_\pi + \overline{\omega}_0 - 2\omega\,. \tag{29}$$

Using the simulated results in Table 1, we have $\Delta f_c = \Delta\omega_c/(2\pi) = -354$ kHz and $Q_{L,c} = \omega_c/(2\alpha_c) = 52.6$.

Table 1: Simulated Results of Eigenmodes

Mode μ	$(\overline{\omega}_\mu - \omega)/(2\pi)$	$Q_{L,\mu} = \overline{\omega}_\mu/(2\alpha_\mu)$
0	−3.397 MHz	100
$\pi/2$	+0.003 MHz	1.57×10^4
π	+3.043 MHz	111

† $\omega/(2\pi) = 508.877$ MHz

Table 2: Parameters of the A- and S-cavities

Parameter	Value
$\Delta f_a = \Delta\omega_a/(2\pi)$	0 MHz
$\Delta f_s = \Delta\omega_s/(2\pi)$	0 MHz
Q_a	29400
Q_s	174000
β_s	10.7
k_a^2/k_s^2	7.619

From Eq. (24) with the parameters in Table 1, we have

$$k_s^2 + k_a^2 = 2.502 \times 10^{-4}\,. \tag{30}$$

From Eqs. (27) and (30), k_s and k_a are derived as

$$k_s = 0.539 \times 10^{-2}, \quad k_a = 1.487 \times 10^{-2}\,. \tag{31}$$

CHARACTERISTIC EQUATION

We checked the obtained values of k_s and k_a using the characteristic equation of the ARES cavity in Eq. (10). Figure 4 shows the numerical solutions of the 6th-order characteristic equation of the ARES cavity. The upper figure shows the resonant frequency $\overline{f}_\mu = \overline{\omega}_\mu/(2\pi)$ and the lower one shows the loaded Q $Q_{L,\mu}$ for the μ mode. These values shown by solid lines correlate with the real and imaginary parts of complex solutions $D(s_\mu) = 0$ as

$$s_\mu = -\frac{\overline{\omega}_\mu}{2Q_{L,\mu}} + j\overline{\omega}_\mu\,, \quad \overline{\omega}_\mu > 0\,. \tag{32}$$

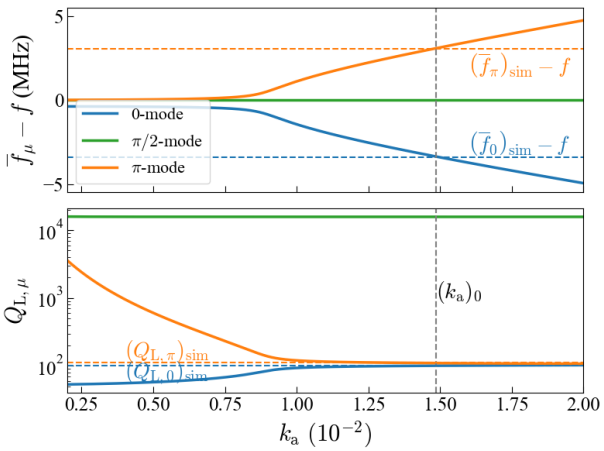

Figure 4: Solutions of the characteristic equation with $\Delta f_c = -354$ kHz and $Q_{L,c} = 52.6$.

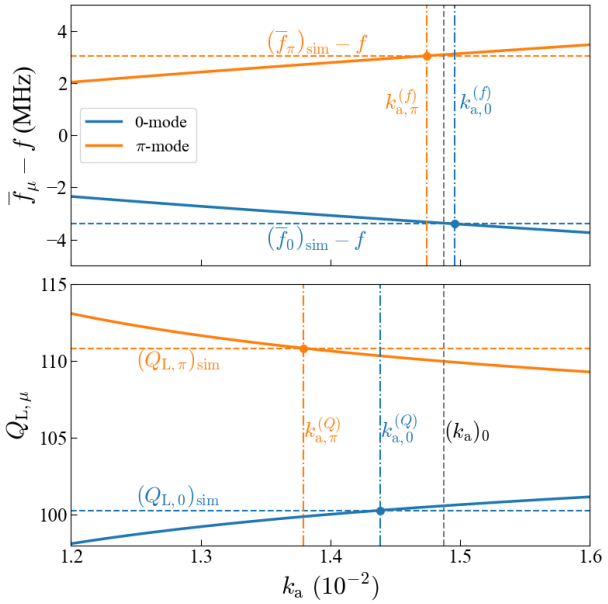

Figure 5: Solutions of the characteristic equation with $\Delta f_{\rm c} = -354$ kHz and $Q_{\rm L,c} = 52.6$.

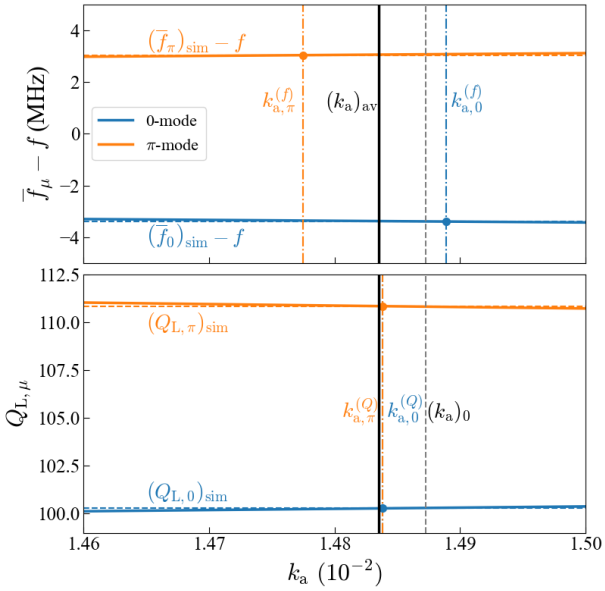

Figure 6: Solutions of the characteristic equation with $\Delta f_{\rm c} = -387$ kHz and $Q_{\rm L,c} = 52.8$.

In Fig. 4, we do not plot the solutions with negative imaginary parts s^*_μ. The parameters assumed for the S- and A-cavities are shown in Table 2. Those were evaluated by eigenmode simulations. For the C-cavity parameters, we used the estimated values from Eqs. (28) and (29). The mode frequencies and loaded Q's are plotted as the functions of $k_{\rm a}$. Here, as changing $k_{\rm a}$, we also changed $k_{\rm s}$ with keeping the ratio $k_{\rm a}^2/k_{\rm s}^2 = 7.619$ in Eq. (27).

The vertical dashed gray line shows $k_{\rm a} = (k_{\rm a})_0$ that indicates the $k_{\rm a}$ value in Eq. (31), and Fig. 5 shows a zoomed plot around $k_{\rm a} = (k_{\rm a})_0$. The horizontal dashed blue lines show the mode frequency $(\overline{f}_\mu)_{\rm sim}$ and loaded Q $(Q_{{\rm L},\mu})_{\rm sim}$ of $\mu = 0$ mode obtained by eigenmode simulations, and the orange lines show those of $\mu = \pi$ mode. In Fig. 5, $k^{(f)}_{{\rm a},\mu}$ $(\mu = 0, \pi)$ shown with dash-dotted lines indicates the $k_{\rm a}$ values at which the simulated frequency $(\overline{f}_\mu)_{\rm sim} - f$ coincides with the solution of the characteristic equation, and $k^{(Q)}_{{\rm a},\mu}$ $(\mu = 0, \pi)$ is similarly defined for loaded Q's. Ideally, $k^{(f)}_{{\rm a},\mu}$ and $k^{(Q)}_{{\rm a},\mu}$ $(\mu = 0, \pi)$ should agree with each other. However, we found that $k^{(f)}_{{\rm a},\mu}$ and $k^{(Q)}_{{\rm a},\mu}$ deviate with $(k_{\rm a})_0$ by maximally 7%. This deviations should come from the errors of approximations in Eqs. (22) and (23).

To obtain more precise results, we adjusted the $\Delta f_{\rm c}$ and $Q_{\rm L,c}$ so that the following function takes minimum:

$$F_k = \left(k^{(f)}_{{\rm a},0} - k^{(f)}_{{\rm a},\pi}\right)^2 + \left(k^{(f)}_{{\rm a},0} - k^{(Q)}_{{\rm a},0}\right)^2 + \left(k^{(f)}_{{\rm a},0} - k^{(Q)}_{{\rm a},\pi}\right)^2 + \left(k^{(f)}_{{\rm a},\pi} - k^{(Q)}_{{\rm a},0}\right)^2 + \left(k^{(f)}_{{\rm a},\pi} - k^{(Q)}_{{\rm a},\pi}\right)^2 + \left(k^{(Q)}_{{\rm a},0} - k^{(Q)}_{{\rm a},\pi}\right)^2 . \quad (33)$$

Here, $F_k = 0$ when all $k^{(f)}_{{\rm a},\mu}$ and $k^{(Q)}_{{\rm a},\mu}$ are equivalent. Using `scipy.optimize.minimize` [10], one of the functions provided by SciPy library for minimizing F_k, the optimized parameters were $\Delta f_{\rm c} = -387$ kHz and $Q_{\rm L,c} = 52.8$. Under these parameters, the solutions of the characteristic equation and $k^{(f)}_{{\rm a},\mu}$ and $k^{(Q)}_{{\rm a},\mu}$ are shown in Fig. 6. The vertical solid black line shows $(k_{\rm a})_{\rm av}$ that is the average value of $k^{(f)}_{{\rm a},0}$, $k^{(f)}_{{\rm a},\pi}$, $k^{(Q)}_{{\rm a},0}$, and $k^{(Q)}_{{\rm a},\pi}$. Comparing Figs. 5 and 6, we can confirm that their deviation are much reduced after the optimization. The maximum deviation of $k^{(f)}_{{\rm a},\mu}$ and $k^{(Q)}_{{\rm a},\mu}$ from $(k_{\rm a})_{\rm av}$ is 0.4%. Identifying $(k_{\rm a})_{\rm av}$ as the realistic $k_{\rm a}$ for the simulation model of the ARES cavity, we obtain

$$\begin{aligned} k_{\rm s} &= (k_{\rm a})_{\rm av}/\sqrt{7.619} = 0.537 \times 10^{-2}, \\ k_{\rm a} &= (k_{\rm a})_{\rm av} = 1.484 \times 10^{-2}\,. \end{aligned} \quad (34)$$

Comparing with Eq. (31), the changes in $k_{\rm s}$ and $k_{\rm a}$ before and after optimizing the parameters of the C-cavity were less than 0.3%. Because $\Delta f_{\rm c}$ was mainly adjusted by optimization, the main cause of deviation of $k_{\rm a}$ values in Fig. 5 would be the $\Delta f_{\rm c}$ estimation in Eq. (29).

CONCLUSION

We developed an evaluation method of the inter-cavity coupling factors for the ARES cavity. Analysing the characteristic equation of the ARES cavity, we derived an analytical method of determining the inter-cavity coupling factors from electromagnetic eigenmode simulations. Simulating the complex eigenfrequencies of the 0, $\pi/2$, and π modes using CST Eigenmode Solver and analysing them, we determined the values $k_{\rm s}$ and $k_{\rm a}$. We confirmed that the numerical solutions of the characteristic equation is consistent with the eigenmode simulation results under the obtained $k_{\rm s}$ and $k_{\rm a}$ after adjusting the C-cavity parameters. Using the accurate values of $k_{\rm s}$ and $k_{\rm a}$, we are going to reconsider some issues such as the transient beam loading effects [11] and C-damper power leak of $\pi/2$ mode.

REFERENCES

[1] Y. Yamazaki and T. Kageyama, "A three-cavity system which suppresses the coupled-bunch instability associated with the accelerating mode", *Part. Accel.*, vol. 44, p. 107, 1994. https://cds.cern.ch/record/251884/files/p107.pdf

[2] K. Akai, N. Akasaki, E. Ezura, T. Kageyama, H. Mizuno, F. Naito, H. Nakanishi, Y. Takeuchi, Y. Yamazaki, and T. Kobayashi, "Tuning control and transient response of the ARES for KEKB", in *Proc. 5th European Particle Accelerator Conf. (EPAC'96)*, Barcelona, Spain, Jun. 1996, paper WEP046L, pp. 1994–1997.

[3] T. Kageyama, K. Akai, N. Akasaka, E. Ezura, H. Mizuno, F. Naito, H. Nakanishi, H. Sakai, Y. Takeuchi, and Y. Yamazaki, "Development of high-power ARES cavities", in *Proc. 17th Particle Accelerator Conf. (PAC'97)*, Vancouver, Canada, May 1997, pp. 2902–2904.

[4] F. Naito, K. Akai, N. Akasaka, E. Ezura, T. Kageyama, H. Mizuno, H. Nakanishi, Y. Takeuchi, Y. Yamazaki, and T. Kobayashi, "Coupling cavity damper for the ARES", in *Proc. 17th Particle Accelerator Conf. (PAC'97)*, Vancouver, Canada, May 1997, pp. 2977–2979.

[5] R. Klatt, F. Krawczyk, W.-R. Novender, C. Palm, T. Weiland, B. Steffen, T. Barts, M. J. Browman, R. Cooper, C. T. Mottershead, G. Rodenz, and S. G. Wipf, "MAFIA - a three-dimensional electromagnetic CAD system for magnets, RF structures, and transient wake-field calculations", in *Proc. 13th Linear Accelerator Conf. (LINAC'86)*, Stanford, California, USA, Jun. 1986, paper WE3-13, pp. 276–278.

[6] CST Studio Suite, https://www.3ds.com/products/simulia/cst-studio-suite

[7] T. Yamaguchi, T. Kobayashi, T. Abe, T. Okada, S. Ogasawara, M. Nishiwaki, S. Enomoto, and J. Zepeda, "Simulation study on power loss in the coupling cavity damper of the accelerating $\pi/2$ mode for the SuperKEKB ARES cavity", in *Proc. 16th International Particle Accelerator Conf. (IPAC'25)*, Taipei, Taiwan, Jun. 2025, paper WEPS059, pp. 2366–2369.
doi:10.18429/JACoW-IPAC25-WEPS059

[8] T. Kobayashi and K. Akai, "Advanced simulation study on bunch gap transient effect", Phys. Rev. Accel. Beams, vol. 19, p. 062001, 2016.
doi:10.1103/PhysRevAccelBeams.19.062001

[9] D. E. Nagle, E. A. Knapp, and B. C. Knapp, "Coupled resonator model for standing wave accelerator tanks", Rev. Sci. Instrum., vol. 38, pp. 1583–1587, 1967.
doi:10.1063/1.1720608

[10] SciPy documentation, https://docs.scipy.org/doc/scipy/reference/generated/scipy.optimize.minimize.html

[11] T. Kobayashi, T. Abe, and T. Yamaguchi, "Present situation of transient beam loading in SuperKEKB acceleration cavity", the Annual Meeting of Particle Accelerator Society of Japan, Tokyo, Japan, Aug. 2025, THP053, this meeting.